AD-A140 586 LOW FREQUENCY ELECTRIC AND MAGNETIC NOISE ALONG THE AURORAL FIELD LINES..(U) IOWA UNIV IOWA CITY DEPT OF PHYSICS AND ASTRONOMY D A GURNETT ET AL. FEB 84 1/1

UNCLASSIFIED U. OF IOWA-84-2 N00014-76-C-0016 F/G 4/1 NL

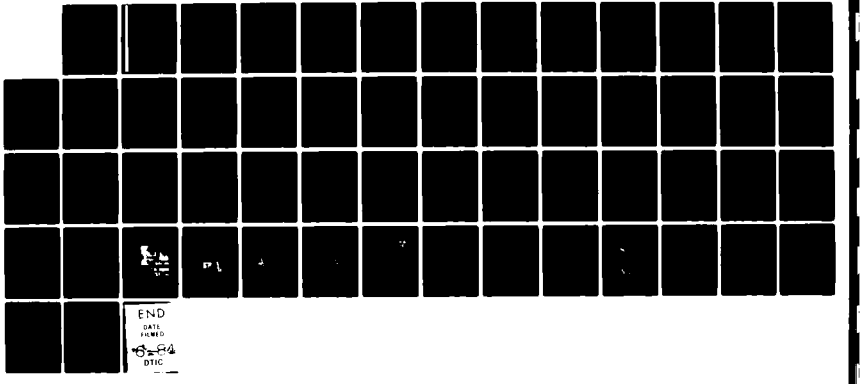

END

DATE FILMED

DTIC

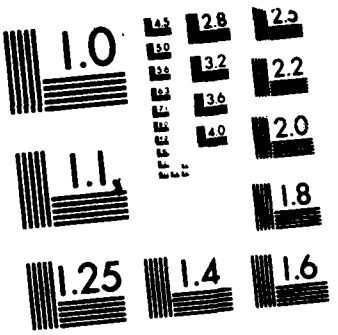

U. of Iowa 84-2

LOW FREQUENCY ELECTRIC AND MAGNETIC NOISE ALONG THE AURORAL FIELD LINES

by

D. A. Gurnett, R. L. Huff, J. D. Menietti,
J. D. Winningham, J. L. Burch, and S. D. Shawhan

Department of Physics and Astronomy
THE UNIVERSITY OF IOWA
Iowa City, Iowa 52242

U. of Iowa 84-2

LOW FREQUENCY ELECTRIC AND MAGNETIC NOISE ALONG THE AURORAL FIELD LINES

by

D. A. Gurnett[1], R. L. Huff[1], J. D. Menietti[2],
J. D. Winningham[2], J. L. Burch[2], and S. D. Shawhan[3]

February 1984

[1]Department of Physics and Astronomy
The University of Iowa
Iowa City, IA 52242

[2]Southwest Research Institute
P. O. Drawer 28510
San Antonio, TX 78284

[3]NASA Headquarters
400 Maryland Ave.
Washington, DC 20546

Submitted for publication to Journal of Geophysical Research.

The research at the University of Iowa was supported by NASA through grant NAG5-310 from Goddard Space Flight Center, through grants NGL-16-001-002 and NGL-16-001-043 from NASA Headquarters, and by the Office of Naval Research through grant N00014-76-C-0016. The research at Southwest Research Institute was supported by NASA through contracts NAS5-26363 and NAS5-25693 from Goddard Space Flight Center and by AFGL through contract AFGL 712183N0001.

UNCLASSIFIED

SECURITY CLASSIFICATION OF THIS PAGE (When Data Entered)

REPORT DOCUMENTATION PAGE		READ INSTRUCTIONS BEFORE COMPLETING FORM
1. REPORT NUMBER U. of Iowa-84-2 ✓	2. GOVT ACCESSION NO.	3. RECIPIENT'S CATALOG NUMBER
4. TITLE (and Subtitle) LOW FREQUENCY ELECTRIC AND MAGNETIC NOISE ALONG THE AURORAL FIELD LINES		5. TYPE OF REPORT & PERIOD COVERED Progress, February 1984 6. PERFORMING ORG. REPORT NUMBER
7. AUTHOR(s) D. A. GURNETT, R. L. HUFF, J. D. MENIETTI, J. D. WINNINGHAM, J. L. BURCH, AND S. D. SHAWHAN		8. CONTRACT OR GRANT NUMBER(s) N00014-76-C-0016
9. PERFORMING ORGANIZATION NAME AND ADDRESS Department of Physics and Astronomy The University of Iowa Iowa City, IA 52242		10. PROGRAM ELEMENT, PROJECT, TASK AREA & WORK UNIT NUMBERS
11. CONTROLLING OFFICE NAME AND ADDRESS Electronics Program Office Office of Naval Research Arlington, VA 22217		12. REPORT DATE February 1984 13. NUMBER OF PAGES 40
14. MONITORING AGENCY NAME & ADDRESS(if different from Controlling Office)		15. SECURITY CLASS. (of this report) UNCLASSIFIED 15a. DECLASSIFICATION/DOWNGRADING SCHEDULE

16. DISTRIBUTION STATEMENT (of this Report)

Approved for public release; distribution is unlimited.

17. DISTRIBUTION STATEMENT (of the abstract entered in Block 20, if different from Report)

18. SUPPLEMENTARY NOTES

Submitted for publication to J. Geophys. Res.

19. KEY WORDS (Continue on reverse side if necessary and identify by block number)

Low frequency waves
Alfven waves
Ion cyclotron waves
DE

20. ABSTRACT (Continue on reverse side if necessary and identify by block number)

(See following pages.)

DD FORM 1 JAN 73 1473 EDITION OF 1 NOV 65 IS OBSOLETE
S/N 0102-LF-014-6601

UNCLASSIFIED

SECURITY CLASSIFICATION OF THIS PAGE (When Data Entered)

ABSTRACT

Plasma wave and plasma measurements from the DE-1 spacecraft are used to investigate an intense band of low frequency, < 100 Hz, electric and magnetic noise detected at low altitudes over the auroral zones. This noise is observed by DE-1 on essentially every low altitude pass over the auroral zone and occurs in regions of intense low energy, 100 eV to 10 keV, electron precipitation and field-aligned currents. The electric field polarization in a plane perpendicular to the static magnetic field is random. Correlation measurements between the electric and magnetic fields show that the perpendicular (approx $\hat{\sim}$ north-south) electric field fluctuations are closely correlated with the perpendicular (east-west) magnetic field fluctuations, and that the Poynting flux is directed downward, toward the Earth. The total electromagnetic power flow associated with these fluctuations is very large, approx 10 to the 8th power watts.

Two interpretations of the low frequency noise are considered: first, that the noise is produced by quasi-static fields imbedded in the ionosphere, and second, that the noise is due to Alfven waves propagating along the auroral field lines. For the quasi-static interpretation, the ratio of the magnetic to electric field strengths is determined by the Pedersen conductivity at the base of the ionosphere, whereas for the Alfven wave interpretation it is determined by the Alfven index of refraction. Measurements show that the magnetic to electric field ratio decreases rapidly with increasing height, in good

agreement with the Alfven wave interpretation and in poor agreement with the quasi-static interpretation. The DE-1 observations therefore provide strong evidence that the low frequency electromagnetic noise is caused by Alfven waves propagating along the auroral field lines. At present, the origin of the Alfven wave turbulence has not been established. Most likely the source is located at high altitudes, since the Poynting flux is usually directed downward toward the Earth at altitudes up to at least 1 R_E.

I. INTRODUCTION

One of the most prominent and commonly occurring types of noise detected by the plasma wave instrument on the Dynamics Explorer 1 spacecraft is an intense, broadband, $f \lesssim 100$ Hz, spectrum of electric and magnetic fluctuations at low altitudes over the auroral zones. The DE-1 observations of this noise are not new. The existence of intense low frequency electric field fluctuations at altitudes of a few thousand km over the auroral zones was first reported by Heppner [1969] using electric field measurements from the OV1-10 spacecraft. This noise was subsequently described and studied by a number of investigators, including Maynard and Heppner [1970], Kelley and Mozer [1972], Kintner [1976], Temerin [1978], Maynard et al. [1982] and Curtis et al. [1982]. Typically the noise occurs over a frequency range from a few Hz to several hundred Hz, decreasing in intensity with increasing frequency. Somewhat similar broadband electric field noise was also reported by Gurnett and Frank [1977] along the auroral field lines at altitudes of several Earth radii and higher. However, because of the markedly different plasma parameters at these higher altitudes it has never been clear that the broadband electrostatic noise observed at high altitudes is the same as the noise observed at lower altitudes.

It has been widely believed that the frequency spectrum of the low altitude electric field noise is caused by the motion of the spacecraft through quasi-static electric field structures in the ionosphere. This

interpretation was first proposed by Heppner [1969] and has been given strong support by Temerin [1978] on the basis of short wavelength antenna interference effects observed in the spectrum of the low frequency noise. These interference effects demonstrate that the wavelengths of the noise can be very short, only a few tens of meters, or less. Wavelengths in this range produce Doppler shifts of several hundred Hz or more at typical spacecraft velocities.

Irregular magnetic field fluctuations are also a common feature of low altitude satellite magnetic field measurements in the auroral zone [Zmuda and Armstrong, 1974a,b]. At low frequencies, below a few tens of Hz, these magnetic field fluctuations are usually interpreted as being due to the motion of the spacecraft through a system of quasi-static field-aligned currents linking the auroral zone and the distant magnetosphere. For a recent review of field-aligned currents in the auroral regions, see Potemra [1983]. Using data from the Hawkeye 1 spacecraft, Kintner [1976] showed that the electric field noise and the magnetic field noise occur in the same region and that both types of noise have similar spectrums, varying approximately as $f^{-1.9}$ for the electric field and as $f^{-2.8}$ for the magnetic field. The noise also occurs in regions of large shear in the east-west convection velocity. These observations led Kintner to suggest that the noise is two-dimensional MHD turbulence excited by a shear-driven instability in the auroral zone. For a further discussion of two-dimensional MHD turbulence processes in the auroral regions, see Kelley and Kintner [1978].

In this paper we describe the DE-1 observations of the low frequency auroral zone noise and discuss the relationship of these observations to low energy plasma measurements on the same spacecraft. Compared to previous observations the DE-1 plasma wave measurements provide a new capability for determining the correlation between various components of the electric and magnetic field, thereby giving new information on the character of the noise. The DE-1 data also provide measurements over a range of altitudes along the auroral field lines that have not been previously surveyed. For a description of the plasma wave instrument on DE-1, see Shawhan et al. [1981] and for a description of the plasma instrument, see Burch et al. [1981].

II. BASIC CHARACTERISTICS AND REGION OF OCCURRENCE

To illustrate the general characteristics of the low frequency electric and magnetic field noise, we will now describe some representative events and discuss the region of occurrence of the noise. A typical example is shown in Figure 1. The top panel of this illustration shows a frequency-time spectrogram of the electric field detected by DE-1 during a low altitude pass over the southern polar region on October 23, 1981. The bottom panel shows the corresponding magnetic field spectrogram. To interpret these spectrograms, it is necessary to understand the geometry of the orbit. DE-1 is in a highly eccentric polar orbit with an apogee geocentric radial distance of 4.65 R_E and a perigee geocentric radial distance of 1.1 R_E. At the time of the pass shown in Figure 1 the perigee was located over the southern polar region. Because of the high spacecraft velocity near perigee, the spacecraft passes over the southern polar region very quickly. The spacecraft crosses through the evening auroral zone from about 0428 to 0433 UT, passes over the polar cap from about 0433 to 0440 UT, and crosses through the morning auroral zone from about 0440 to 0444 UT. The dark portions of the spectrogram indicate regions of higher intensity. The low frequency electric and magnetic field noise is clearly evident over the evening and morning auroral zones at frequencies extending up to about 50 Hz.

Usually the low frequency electric and magnetic field noise is most intense in the lowest, 1.78 Hz, frequency channel and decrease in intensity with increasing frequency. The noise sometimes has an upper frequency limit near the cyclotron frequency of singly charged oxygen, O^+. For reference, the cyclotron frequencies for protons, f_{cH+}, and singly charged oxygen, f_{cO+}, are shown in Figure 1. As can be seen, most of the energy in the spectrum is concentrated below the O^+ cyclotron frequency. The tendency for the electric field spectrum to have an upper frequency limit near f_{cO+} has been previously pointed out by Curtis et al. [1982]. Although the noise sometimes appears to have a cutoff near the O^+ cyclotron frequency, cases can be found where the spectrum extends well above f_{cO+}. This is particularly true for the electric field. For example, during the morning auroral zone crossing in Figure 1, from 0440 to 0444 UT, the electric field spectrum can be seen extending up to near the proton cyclotron frequency. Often the higher frequency noise is of entirely different origin, either auroral hiss emissions or ELF noise bands of the type reported by Gurnett and Frank [1972], and Temerin and Lysak [1984]. With the available frequency resolution it is often difficult to determine the transition between these different types of noises.

Another example of the low frequency electric and magnetic noise is shown in Figure 2. This illustration shows a magnetic field spectrogram from a pass over the southern polar cap on January 11, 1982, about three months after the pass in Figure 1. The low frequency noise

is again clearly evident over the two auroral zones, from 0838 to 0843 UT in the local evening, and from 0846 to 0849 UT in the local morning. The tendency for the spectrum to exhibit a cutoff near the O^+ cyclotron frequency is again evident. Examination of all the passes that occurred during this period shows that the low frequency noise persists with very similar characteristics from one orbit to the next over a period of at least several months. The width of the region of enhanced noise levels and the peak intensities vary somewhat from orbit to orbit, but the noise is essentially always detectable.

To determine the region of occurrence of the low frequency noise, a survey was performed of all of the DE-1 spectrograms obtained over a two-year period, from September 1981 to September 1983. The criterion for identifying the noise was to select events with simultaneous broadband electric and magnetic field spectrums comparable to those shown in Figures 1 and 2. The results of this survey are shown in Figures 3 and 4. Figure 3 shows the spacecraft trajectory for all of the events identified plotted as a function of radial distance and magnetic latitude. It is evident that the noise occurs at all altitudes along the auroral field lines up to radial distances of at least 2 R_E. Usually, the intensity and upper frequency limit of the magnetic noise decreases with increasing altitude. The electric field spectrum is more complicated and tends to spread upward in frequency with increasing altitude, merging into a broadband spectrum characteristic of the broadband electrostatic noise described by Gurnett and Frank [1977]. The region of occurrence in Figure 3 does not extend to the higher altitudes reported

by Gurnett and Frank [1977] because we demanded the simultaneous presence of both electric and magnetic noise. Since the broadband electrostatic noise is quite common at higher altitudes, the upper altitude cutoff of the events in Figure 3 is mainly determined by the magnetic noise.

The distribution of the low frequency noise in magnetic local time and invariant latitude is shown in Figure 4. Except for gaps in the early morning and early afternoon, the noise occurs at essentially all local times around the auroral zone. The gaps in the early morning and early afternoon are believed to be a sampling effect caused by secular changes in the orbit. Because of the combined effect of the latitudinal motion of perigee and the change in the local time of the orbit plane, no low altitude passes are available in the present data set in the early morning and early afternoon.

III. RELATIONSHIP TO AURORAL PRECIPITATION

To establish the relationship between the low frequency electric and magnetic noise and the auroral zone, we have investigated the DE-1 plasma measurements for a number of the events described in the previous section. A typical example is shown in Figure 5. The top panel of this illustration shows the magnetic field spectrogram for a low altitude pass over the southern polar region on October 25, 1981, two days after the event shown in Figure 1. Again the low frequency noise can be identified in the two auroral zones, from 0425 to 0428 UT in the local evening, and from 0434 to 0439 UT in the local morning. For comparison the low energy electron flux, electron density, and field-aligned current density are shown in the bottom three panels, which are expanded to cover the time interval from 0424 to 0442 UT. These parameters were obtained by integrating over electron energies from 56 to 13,206 eV. The regions of intense low frequency noise are indicated by shading. Well-defined enhancements in the electron flux and electron density are evident in the region where the noise is observed. The low energy electron fluxes, $\sim 10^{9}$ to 10^{10} cm^{-2} sec^{-1}, and electron densities, $\sim 10^{-1}$ to 1.0 cm^{-3}, are typical of the electron precipitation commonly observed in the auroral regions. Usually little or no proton precipitation is observed in these regions. The bottom panel of Figure 5 shows that the low frequency noise is also closely

associated with regions of enhanced field-aligned current densities. The current densities are computed from the measured electron distribution function, integrated over the energy range, 56 to 13,206 eV. Most of the contribution to the field-aligned current comes from low energy electrons with energies of a few hundred eV.

Another example comparing the low frequency electric and magnetic field noise and the low energy electron measurements is shown in Figure 6. This example is for the pass over the southern polar region shown in Figure 1, on October 23, 1981. The top panel of Figure 6 shows the magnetic field spectral density on an expanded time scale, and the bottom three panels show the electron flux, electron density and field-aligned current density. The regions of intense low frequency noise are indicated by shading. Again the noise is seen to occur only in regions of enhanced electron flux characteristic of the auroral zone. As in the previous example, the noise is again closely related to regions of enhanced field-aligned current density.

IV. ELECTRIC AND MAGNETIC FIELD SPECTRUMS AND CORRELATIONS

To help determine the nature of the plasma fluctuations responsible for the low frequency electric and magnetic noise, we have performed a detailed study of the relationship between the electric and magnetic field spectrums, including correlations between the various field components. Comparisons of two simultaneously measured electric and magnetic field spectrums are shown in Figures 7 and 8. The spectrums in Figure 7 are from the pass on October 23, 1981, shown in Figure 1, and the spectrums in Figure 8 are from the pass on January 11, 1982, shown in Figure 2. Both of the spectrums have been selected from times of maximum intensity during the pass. In both cases the spectrums decrease monotonically with increasing frequency. Although Kintner [1976] has chosen to describe the electric and magnetic field spectrum by a power law, these spectrums show that the intensities often deviate considerably from a power law. We find that the spectrum often has a peak or a change in slope that cannot be accurately described by a power law. Also notable is the tendency for the electric and magnetic field spectrums to have the same shape, particularly at frequencies below about a hundred Hz. If the electric field spectrum has a peak or a change in slope, then this feature is usually also present in the magnetic field spectrum. One is given the strong impression that the electric and magnetic field spectrums are closely related.

To characterize the relationship between the electric and magnetic field spectrums, it is useful to compute the ratio of the magnetic to electric field strength. This ratio is shown as a function of frequency in the top panel of Figures 7 and 8, and is expressed in terms of an index of refraction, $n = cB/E$, on the left, and a conductivity, $\Sigma = B/(\mu_o E)$, on the right. Possible interpretations of these two quantities are discussed in the next section. The magnetic to electric field ratio is usually nearly independent of frequency, as in Figure 7, or decreases slightly with increasing frequency, as in Figure 8. At low altitudes, $R \simeq 1.2\ R_E$, the magnetic to electric field ratio is usually fairly consistent from orbit to orbit, with typical values ranging from $n \simeq 300$ to 1000, and from $\Sigma = 0.5$ to 2.0 mhos. Statistical studies show that the magnetic to electric field ratio decreases systematically with increasing altitude. This variation is illustrated in Figure 9, which shows a scatter plot of cB/E and $B/(\mu_o E)$ as a function of altitude using all of the available data. Two frequencies, 3.11 Hz and 10 Hz are shown. All frequencies below about 100 Hz show the same basic trend, with the magnetic to electric field ratio decreasing with increasing altitude. The scatter in the individual points with respect to the overall trend tends to decrease with increasing frequency. The scatter is also affected by the correlation between the electric and magnetic fields, which can be measured with the on-board correlator, and tends to decrease with increasing correlation coefficient. To reduce the scatter and help eliminate the uncorrelated component of the noise, the points plotted in Figure 9 have been restricted to correlation coefficients, ρ, greater than 0.6. This criterion eliminated about one-half of the data points.

Except for various types of electromagnetic emissions at high frequencies, the magnetic field spectral density usually drops below the instrument noise level at frequencies above a few tens of Hz. In some cases the magnetic field spectrum shows very convincing evidence of a decrease in intensity near the O^+ cyclotron frequency, as in Figure 8. In other cases, as in Figure 7, the evidence of a cutoff at f_{cO+} is less certain, possibly because the spectral density drops to near the instrument noise level before reaching the cutoff. The evidence for a cutoff in the electric field spectrum at the O^+ cyclotron frequency is less convincing. Usually the electric field spectrum is most intense below the O^+ cyclotron frequency, but often a weak component extends across f_{cO+} to higher frequencies. Since whistler mode auroral hiss and other types of electrostatic noise are usually present at higher frequencies, one has the strong impression that two different types of noise may be overlapping in this part of the spectrum.

Further information on the relationship between the low frequency electric and magnetic field noise can be obtained from the correlator incorporated in the DE-1 plasma wave instrument. The correlator gives the correlation coefficient and relative phase between signals received by any selected pair of antennas. An example of the output of the correlator is shown in Figure 10 for a low frequency noise event observed at low altitudes over the southern auroral zone on September 24, 1981. In this case, the correlator was connected to the B_z search coil magnetic antenna and the E_x electric dipole antenna. The B_z antenna is parallel to the spin axis, and the E_x antenna is perpendicular to the spin axis. Since the DE-1 spin axis is perpendicular to the orbital plane the B_z antenna measures the east-west component of

the magnetic field. As the spacecraft rotates the E_x antenna alternately measures the perpendicular (~ north-south) and parallel components of the electric field. The correlation coefficient and relative phase are measured in a narrow frequency band controlled by the stepping of the sweep frequency receiver. During the 32 sec interval shown in Figure 10, the correlator steps through four frequency bands, 1.78 Hz, 3.11 Hz, 5.62 Hz, and 10.0 Hz, each with a bandwidth of about ±15%. The center frequencies of these bands are indicated at the top of Figure 10. The top two panels show the amplitude of the E_x and B_z fields, and the bottom two panels show the relative phase ϕ, and the correlation coefficient ρ, between the E_x and B_z fields. The vertical dashed lines indicate times when the +x antenna axis is parallel to the Earth's magnetic field, $\vec{B}_o$, projected into the spin plane. Because the Earth's magnetic field is usually within a few degrees of the spin plane, the E_x antenna axis is very nearly parallel to the Earth's magnetic field at these times.

Inspection of Figure 10 shows that the E_x amplitude tends to have a minimum when the +x antenna axis is parallel or anti-parallel to the Earth's magnetic field. This spin modulation indicates that the electric field is oriented mainly perpendicular to the magnetic field. No spin modulation is evident in the B_z amplitude because this axis is parallel to the spin axis. The bottom panel of Figure 10 shows that the correlation coefficient between the E_x and B_z fields is large, typically greater than 80%. Roughly twice per rotation the correlation coefficient briefly drops to a low value. These minimums in the

correlation coefficient occur at minimums in the electric field intensity, when the +x antenna axis is parallel or anti-parallel to the Earth's magnetic field. The second panel from the bottom shows that the relative phase between the E_x and B_z fields alternates back and forth between $\phi = 0°$ and $\phi = 180°$, producing a clearly defined square wave pattern. The transitions between $\phi = 0°$ and $\phi = 180°$ occur when the +x antenna axis is parallel or anti-parallel to the Earth's magnetic field. The high correlation coefficient and the square wave phase pattern show that the fluctuations in the perpendicular (east-west) component of the magnetic field and the perpendicular (~ north-south) component of the electric field are highly correlated. Careful consideration of the directions involved shows that the fluctuations are such that the Poynting flux, $\vec{S} = \vec{E} \times \vec{B}/\mu_0$, is directed downward along the magnetic field line, toward the Earth. Investigation of other similar cases always shows the same basic pattern. Although the correlation coefficient is not always as high as shown in Figure 10, it is usually greater than 50%, and whenever a clearly defined square wave pattern is observed in the phase plot, the Poynting flux is directed toward the Earth. By integrating over typical electric and magnetic field spectrums, as in Figure 7 and 8, and using a representative correlation coefficient, the electromagnetic energy flux associated with the noise can be estimated. Integrated from 1 Hz to 100 Hz one finds for a typical event that $E_x \simeq 3\ mVm^{-1}$, $B_z \simeq 10$ nT, and $\rho \simeq 0.8$, which gives $S \simeq 2 \times 10^{-2}$ erg cm^{-2} sec^{-1}. This energy flux is about 0.1 to 1% of the electron energy flux precipitated in the auroral regions.

The polarization of the electric field fluctuations in a plane perpendicular to the magnetic field can be obtained by selecting times when the E_x and E_z electric antennas are connected to the correlator. An example of an event where the electric field polarization can be measured with this technique is shown in Figure 11. Again, clearly defined minimums can be seen in the E_x field amplitude when the +x antenna axis is parallel or anti-parallel to the Earth's magnetic field. No spin modulation is evident in the E_z field amplitude because this antenna axis is parallel to the spin axis. The correlation coefficient between the E_x and E_z fields is again seen to be relatively high, usually exceeding 50%. However, a consistent square wave spin modulation pattern is not evident in the phase plot. The absence of a spin modulation pattern in the phase plot indicates that even though the fields may be correlated on short time scales, the polarization is essentially random on a time scale comparable to the spacecraft rotation period. Other cases investigated show the same result. Therefore, it must be concluded that the polarization of the perpendicular component of the electric field is essentially random. No evidence is found for a consistent right- or left-hand polarization with respect to the Earth's magnetic field. Polarization measurements could not be performed on the magnetic field because only one magnetic sensor is available for magnetic field measurements.

V. POSSIBLE INTERPRETATIONS

Two alternate interpretations can be advanced to explain the correlation between the low frequency electric and magnetic field noise. The noise could be caused by either small scale electrostatic and magnetostatic structures imbedded in the plasma, or by long wavelength electromagnetic waves. In the former interpretation the frequencies observed by the spacecraft would be determined by Doppler shifts, whereas in the latter interpretation the frequencies would be the actual frequencies of the wave. We now consider these two interpretations in detail.

A. Quasi-Static Model

If the low frequency noise is attributed to the motion of the spacecraft through quasi-static electric and magnetic field structures in the ionosphere then the frequency spectrum would be entirely determined by the Doppler shift, $\omega = \vec{k} \cdot \vec{v}$. An upper cutoff frequency near the O^+ cyclotron frequency would then have to be completely coincidental, because the Doppler shift bears no relationship to the cyclotron frequency. For the upper part of the magnetic field spectrum the spatial scale lengths required to explain a Doppler shift of 50 Hz is about 200 meters. This length scale is small, but not unreasonably small for auroral phenomena. Auroral arcs with a thickness of only a few hundred meters have been reported [Akasofu, 1965].

Because of the high conductivity along the magnetic field lines, it is expected that any static structures that exist in the ionosphere would tend to be two-dimensional with the electric and magnetic field fluctuations mainly perpendicular to the static magnetic field. The electric fields would then be associated with field-aligned charge sheets and the magnetic fields would be associated with field-aligned current sheets. If two-dimensional static structures of this type are present in the ionosphere then one may question why the electric and magnetic fields would be so closely correlated. A convenient answer is provided by Smiddy et al. [1980]. If the field-aligned currents close in a meridian plane through the base of the ionosphere, as illustrated in Figure 12, then the north-south electric field is related to the field-aligned current by the height-integrated Pedersen conductivity, Σ_p. It is relatively straightforward to show that $B/(\mu_o E) = \Sigma_p$, where B is the east-west magnetic field and E is the north-south electric field. The correlation between the north-south electric field and the east-west magnetic field and the relation to the Pedersen conductivity has been previously observed and discussed by Sugiura et al. [1982].

It is easy to see by reference to Figure 12 that the fluctuations in the north-south electric field and east-west magnetic field are correlated in such a way that the Poynting flux is directed downward, toward the Earth, in agreement with the observations. The downward direction for the Poynting flux arises because energy is being dissipated by Joule heating at the base of the ionosphere. The origin of the energy required to drive this dissipation is not addressed by

the basic model. The fact that the average Poynting flux is downward at altitudes up to several thousand km indicates that the energy source is located above this altitude range. Several possible energy sources can be identified. If the perpendicular electric field structures are produced by a shear driven instability, as suggested by Kintner [1976] and Kelley and Kintner [1978], then the energy would come from the shear in the convective plasma flow. On the other hand, the spatial structure could also be related to a boundary condition imposed by double-layers or electrostatic shocks at high altitudes. Mozer [1981] has described electrostatic shocks at altitudes of several R_E that map to transverse scales lengths as small as 100 meters in the ionosphere.

The static structure model can be tested by comparing the measured magnetic to electric field ratios to the Pedersen conductivity. Near the base of the ionosphere $B/(\mu_o E)$ should agree with the Pedersen conductivity. From the scatter plot in Figure 9, and from the individual cases in Figures 7 and 8, it can be seen that the magnetic to electric field ratios measured at low altitudes correspond to a conductivity typically in the range from about 0.5 to 2 mho. These conductivities are significantly smaller than the typical height-integrated Pedersen conductivies of 8 to 20 mhos measured in diffuse auroras and discrete arcs by Horwitz et al. [1978] using radar backscatter techniques. Comparisons can also be made in the specific cases by computing the Pedersen conductivity from the measured electron precipitation using the procedures of Wallace and Budzinski [1981] and Spiro et al. [1982]. For the spectrum in Figure 7 the Pedersen conductivity computed from

the precipitated electron spectrum was $\Sigma_p = 4.7$ mhos. This value is higher than the conductivity determined from the magnetic to electric field ratio. However, considering the uncertainties involved the computed conductivity may still be within an acceptable range. For example, for spatial scales less than a few hundred meters the current should start to close in the upper part of the conducting layer, thereby reducing the effective conductivity (C. Goertz, personal communication). Short wavelength corrections of this type will require further study.

To compare the Pedersen conductivity with magnetic to electric field ratios measured at higher altitudes it is necessary to adopt a model for mapping the electric and magnetic fields to higher altitudes. If it is assumed that the parallel electric field is zero and that the current responsible for the magnetic field is field-aligned, then it is easy to show that the magnetic to electric field ratio is given by

$$\frac{B}{(\mu_o E)} = \Sigma_p \left(\frac{1 + 3 \sin^2 \lambda_m}{1 + 3 \sin^2 \Lambda}\right)^{1/2} , \qquad (1)$$

where λ_m is the magnetic latitude and Λ is the invariant latitude. Near the Earth, where $\lambda_m \simeq \Lambda$, the magnetic to electric field is nearly independent of radial distance. This prediction is in strong disagreement with the observed radial dependence of $B/(\mu_o E)$ shown in Figure 9. Thus, the simple static structure model of Smiddy et al. [1980] is not

able to account for an essential feature of the observations. The only way that a quasi-static model could account for the observed radial dependence of $B/(\mu_o E)$ is for a non-zero parallel electric field to be present. Parallel electric fields are of course thought to be present in the auroral regions. To determine the electric field mapping in the presence of a parallel electric field requires a specific model for the parallel electric field. Such models exist. See, for example, Lyons [1980]. However, these models mainly deal with large-scale fields and do not provide predictions that can be easily compared with the radial variation of $B/(\mu_o E)$ shown in Figure 9. Therefore, further study will be needed before a definitive comparison can be made.

B. Alfven Wave Model

If the electric and magnetic fields of the low frequency noise is attributed to long wavelength electromagnetic waves then we must identify the mode of propagation. For frequencies below the ion cyclotron frequency, the only possibility is an Alfven mode, since no other electromagnetic mode exists in this frequency range. The possibility of Alfven waves propagating along the auroral field lines has been suggested by several investigators, including for example Scholer [1970], Goertz and Boswell [1979], and Lysak and Dum [1983]. If a disturbance is imposed on the auroral field lines at large distances from the Earth, this disturbance is transmitted along the field line as an Alfven wave. It is easy to verify that for a source at several R_E the round trip travel time for an Alfven wave through the ionosphere and back to the source is several seconds. For typical convection

speeds of a few km/sec, the plasma will have moved several km by the time a disturbance imposed by the source has propagated to the base of the ionosphere and back. Therefore, for spatial scales of a few km or less, it is necessary to take into account the propagation and reflection of Alfven waves between the source and the base of the ionosphere. This situation is somewhat analogous to the propagation of waves in a transmission line. To arrive at a steady-state equilibrium the magnetic and electric fields must undergo a complex time-dependent oscillation between the values determined by the resistive load, $B/E = \mu_o \Sigma_p$, and the value determined by the Alfven index of refraction, $B/E = n_A/c$.

The Alfven wave interpretation can be tested by comparing the magnetic to electric field ratio, cB/E, with the Alfven index of refraction, $n_A = \sqrt{\rho_m}/(\varepsilon_o B_o)$, where ρ_m is the mass density and B_o is the static magnetic field strength. For Alfven waves propagating parallel to the Earth's magnetic $cB/E = n_A$. For other propagation angles cB/E is proportional to n_A. As can be seen from Figures 7 and 8, at low altitudes cB/E ranges from about 500 to 1000. For a plasma consisting of O^+ ions, which should be the dominant ion at low altitudes, the electron density would have to be in the range from about 6×10^5 to 1.5×10^5 cm^{-3}. These values are very typical of the electron densities in the topside auroral ionosphere at $R = 1.1$ to 1.2 R_E [Nelms, 1966]. Thus, at low altitudes the observed magnetic to electric field ratios are in good agreement with an Alfven wave interpretation.

To carry out a meaningful comparison at higher altitudes we must investigate the radial variation of the Alfven index of refraction.

The basic radial dependence is well-established. Near the Earth the index of refraction should decrease exponentially with increasing altitude because of the exponential altitude variation of the O^+ plasma density. At higher altitudes, beyond about 1.5 to 2.0 R_E, the index of refraction profile should level off and then start to increase as the plasma composition changes from O^+ to H^+. Qualitatively this radial dependence is in good agreement with the measured cB/E ratios in Figure 9. To conduct a quantitative comparison a specific plasma density model is needed. Near the Earth, at altitudes below a few thousand km, the plasma density has been extensively studied by low altitude polar orbiting spacecraft. For example, see Chan and Colin [1969], or Brace [1970]. Farther from the Earth fewer measurements are available and the density profile is less well known. Recently, a study of the electron density profile over the polar region has been carried out by Persoon et al. [1983], using data from DE-1. Although this study was restricted to the polar cap, comparisons in specific cases show that the density in the auroral regions is usually lower than the polar cap densities by about a factor of two or three. Using the density profile obtained by Persoon et al. [1983] at high altitudes, and the densities measured by Chan and Colin [1969] at low altitudes, the model shown in Figure 13 has been constructed. The shaded region marked "Alfven wave model" indicates the estimated range of n_A values. The wide range of uncertainty at high altitudes is due to the unknown composition at high altitudes. The upper limit assumes that the plasma is entirely O^+, and the lower limit assumes a transition from O^+ to H^+ at about 1.4 R_E. Because this is an "average" model, significant deviations can be expected because of seasonal

effects, auroral activity, and other factors, particularly at higher altitudes. Considering these uncertainties, the model index of refraction profile is seen to be in good quantitative agreement with the measured cB/E ratios, particularly if the plasma has a substantial O^+ concentration at high altitudes.

Near the ion cyclotron frequency, the left-hand polarized Alfven wave becomes an ion cyclotron wave [Stix, 1962]. Because left-hand polarized ion cyclotron waves do not propagate at frequencies above the ion cyclotron frequency, this propagation cutoff could explain why a cutoff sometimes exists at the O^+ cyclotron frequency. The possibility that the low frequency noise consists partly of left-hand polarized waves may have some interesting implications for ion heating in the auroral regions. Although the average energy flow is directed toward the Earth, a substantial amount of the wave energy should be reflected from the ionosphere, as illustrated in Figure 14. As the reflected wave propagates upward, the left-hand polarized component will be absorbed by O^+ ions at the O^+ cyclotron frequency. Because the wave energy integrated over the auroral zones (2×10^{-2} ergs cm^{-2}, over an area of 2 × 500 km × 6000 km) is very large, approximately 1.2×10^8 watts, the energy input into the O^+ ions could be appreciable. This heating could possibly account for the upflowing O^+ conics reported by Collins et al. [1983] and Yau et al. [1984]. Rough estimates by Yau [personal communication] indicate that a total power of about 5×10^7 watts is required to account for the outflowing O^+ ions observed during quiet times, increasing to about 1.6×10^8 watts during disturbed times. The possibility of resonant absorption of left-hand polarized ion cyclotron waves as a mechanism for

heating ions is not new. Ion cyclotron waves have been used for ion heating in laboratory plasmas, and Temerin et al. [1984] have already suggested that H^+ electromagnetic ion cyclotron waves could be responsible for producing H^+ ion conics.

IV. CONCLUSION

We have presented DE-1 measurements of intense low frequency electric and magnetic noise observed at low altitudes over the auroral zone. The polarization of the electric field in a plane perpendicular to the Earth's magnetic field is essentially random. Phase measurements show that the transverse electric and magnetic fields are closely correlated, with the average Poynting flux directed downward, toward the Earth. The total power associated with the noise is substantial, approximately 10^8 watts integrated over both auroral zones. The source of this noise must be located along the auroral field lines at altitudes of several thousand km or more.

Two alternative models have been discussed to interpret these observations, one based on quasi-static electric and magnetic fields structures imbedded in the ionosphere, and the other based on the propagation of Alfven waves along the auroral field lines. For the quasi-static model with $E_\parallel = 0$ the magnetic to electric field ratio is determined by the height-integrated Pedersen conductivity at the base of the ionosphere, $B/(\mu_o E) = \Sigma_p$, whereas for the Alfven wave model the magnetic to electric field ratio is determined by the Alfven index of refraction, $cB/E = n_A$. The measured magnetic to electric field ratios are in good quantitative agreement with the Alfven wave model, and in strong disagreement with the quasi-static model. The only way that a quasi-static model could be brought into agreement with the observations is for a parallel electric field to be present along the auroral field lines. At the present time, no suitable theory exists to predict the altitude dependence of the parallel electric field.

Overall, we believe that the DE-1 measurements provide strong evidence of the existence of Alfven wave turbulence along the auroral field lines, mainly because of the close similarity of the measured cB/E ratio with the expected radial variation of the Alfven index of refraction. We do not suggest that Alfven waves account for all of the electric field noise observed in the auroral regions. As shown by Temerin [1978] there is strong evidence of very short wavelength (tens of meters) electrostatic turbulence in the auroral regions. Although the shear Alfven mode can develop a strong electrostatic component at large wave normal angles, such short wavelengths cannot reasonably be interpreted as Alfven waves. Most likely, a mixture of both electromagnetic and electrostatic waves occurs along the auroral field lines. The scatter in the measured magnetic to electric field ratios, and the fact that the scatter is reduced as the correlation coefficient is increased supports this point of view. At the present time we do not know the origin of the Alfven wave turbulence. Possibly the waves could be produced by a shear-driven MHD turbulence process, such as suggested by Kintner [1976], or by a kinetic instability driven by free energy in the auroral electron distribution. We do, however, know that the source is located at relatively high altitudes since the average energy flow is always toward the Earth, even at altitudes up to 1 RE. Whatever the source the total power involved is substantial, at least 10^8 watts. Most of this energy is probably dissipated in the conductive layer at the base of the ionosphere. However, if some of the energy is reflected from the base of the ionosphere, then the reflected waves could possibly play a role in ion acceleration if the left-hand polarized component is absorbed at the ion cyclotron frequency.

ACKNOWLEDGEMENTS

The authors would like to acknowledge useful discussions of the interpretation of these data with L. Brace and N. Maynard of NASA Goddard Space Flight Center and with C. Goertz at the University of Iowa. The research at the University of Iowa was supported by NASA through grant NAG5-310 from Goddard Space Flight Center, through grants NGL-16-001-002 and NGL-16-001-043 from NASA Headquarters, and by the Office of Naval Research through grant N00014-76-C-0016. The research at Southwest Research Institute was supported by NASA through contracts NAS5-26363 and NAS5-25693 from Goddard Space Flight Center and AFGL through contract AFGL 712183N0001.

REFERENCES

Akasofu, S.-I., Dynamic morphology of auroras, Space Sci. Rev., 4, 498, 1965.

Brace, L. H., The global structure of ionospheric temperature, Space Research X, North Holland Publishing Co., Amsterdam, 633, 1970.

Burch, J. L., J. D. Winningham, V. A. Blevins, N. Eaker and W. C. Gibson, High-altitude plasma instrument for Dynamics Explorer-A, Space Sci. Instr., 5, 455, 1981.

Chan, K. L., and L. Colin, Global electron density distributions from topside soundings, Proc. IEEE, 57, 990, 1969.

Collins, H. L., R. D. Sharp, and E. G. Shelley, The magnitude and composition of the outflow of energetic ions from the ionosphere, J. Geophys. Res., submitted, 1983.

Curtis, S. A., W. R. Hoegy, L. H. Brace, N. C. Maynard, and M. Sugiura, DE-2 cusp observations: Role of plasma instabilities in topside ionospheric heating and density fluctuations, Geophys. Res. Lett., 9, 997, 1982.

Goertz, C. K., and R. W. Boswell, Magnetosphere-ionosphere coupling, J. Geophys. Res., 84, 7239, 1979.

Gurnett, D. A., and L. A. Frank, ELF noise bands associated with auroral electron precipitation, J. Geophys. Res., 77, 3411, 1972.

Gurnett, D. A., and L. A. Frank, A region of intense plasma wave turbulence on auroral field lines, J. Geophys. Res., 82, 1031, 1977.

Heppner, J. P., Magnetospheric convection patterns inferred from high latitude activity, Atmospheric Emissions, ed. by B. M. McCormac and A. Omholt, Reinhold Publishing Co., Dordrecht, Holland, 251, 1969.

Horwitz, J. L., J. R. Doupnik, and P. M. Banks, Chatanika radar observations of the latitudinal distributions of auroral zone electric fields, conductivities, and currents, J. Geophys. Res., 83, 1463, 1978.

Kelley, M. C., and P. Kintner, Two-dimensional turbulence in a low β cosmic scale plasma, Astrophys. J., 220, 339, 1978.

Kelley, M. C., and F. S. Mozer, A satellite survey of vector electric fields in the ionosphere at frequencies of 10 to 500 Hz, 1. Isotropic, high-latitude electrostatic emissions, J. Geophys. Res., 77, 4158, 1972.

Kintner, P. M., Jr., Observations of velocity shear driven plasma turbulence, J. Geophys. Res., 81, 5114, 1976.

Lyons, L. R., Generation of large-scale regions of auroral currents, electric potentials, and precipitation by the divergence of the convection electric field, J. Geophys. Res., 85, 17, 1980.

Lysak, R. L., and C. T. Dum, Dynamics of magnetosphere-ionosphere coupling including turbulent transport, J. Geophys. Res., 88, 365, 1983.

Maynard, N. C., and J. P. Heppner, Variations in electric fields from polar orbiting satellites, Particles and Fields in the Magnetosphere, ed. by B. M. McCormac, Reinhold Publishing Co., Dordrecht, Holland, 247, 1970.

Maynard, N. C., J. P. Heppner, and A. Egeland, Intense, variable electric fields at ionospheric altitudes in the high latitude regions as observed by DE-2, Geophys. Res. Lett., 9, 981, 1982.

Mozer, F. S., ISEE 1 observations of electrostatic shocks on auroral field lines between 2.5 and 7 Earth radii, Geophys. Res. Lett., 8, 823, 1981.

Nelms, G. L., Seasonal and diurnal variations of the distribution of electron density in the topside of the ionosphere, Electron Density Profiles in the Ionosphere and Exosphere, ed. by J. Frihagen, North-Holland Publishing Co., Amsterdam, 358, 1966.

Persoon, A. M., D. A. Gurnett, and S. D. Shawhan, Polar cap electron densities from DE 1 plasma wave observations, J. Geophys. Res., 88, 10,123, 1983.

Potemra, T. A., Birkeland currents: Present understanding and some remaining questions, High-Latitude Space Plasma Physics, ed. by B. Hultqvist and T. Hagfors, Plenum Publishing Co., 335, 1983.

Scholer, M., On the motion of artificial ion clouds in the ionosphere, Planet. Space Sci., 18, 977, 1970.

Shawhan, S. D., D. A. Gurnett, D. L. Odem, R. A. Helliwell, and C. G. Park, The plasma wave and quasi-static electric field instrument (PWI) for Dynamics Explorer-A, Space Sci. Instr., 5, 535, 1981.

Smiddy, M., W. J. Burke, M. C. Kelley, N. A. Saflekos, M. S. Gussenhoven, D. A. Hardy, and F. J. Rich, Effects of high-latitude conductivity on observed convection electric fields and Birkeland currents, J. Geophys. Res., 85, 6811, 1980.

Spiro, R. W., P. H. Reiff, and L. J. Maher, Jr., Precipitating electron energy flux and auroral zone conductances--an empirical model, J. Geophys. Res., 87, 8215, 1982.

Stix, T. H., The Theory of Plasma Waves, McGraw-Hill, N. York, 1962.

Sugiura, M., N. C. Maynard, W. H. Farthing, J. P. Heppner, B. G. Ledley, and L. J. Cahill, Jr., Initial results on the correlation between the magnetic and electric fields observed from the DE-2 satellite in the field-aligned current regions, Geophys. Res. Lett., 9, 985, 1982.

Temerin, M., The polarization, frequency, and wavelength of high-latitude turbulence, J. Geophys. Res., 83, 2609, 1978.

Temerin, M., and R. L. Lysak, Electromagnetic ion cyclotron (ELF) waves generated by auroral electron precipitation, J. Geophys. Res., submitted, 1984.

Wallis, D. D., and E. E. Budzinski, Empirical models of height integrated conductivities, J. Geophys. Res., 86, 125, 1981.

Yau, A. W., B. A. Whalen, W. K. Peterson, and E. G. Shelley, Distribution of upflowing ionospheric ions in the high-altitude polar cap and auroral ionosphere, J. Geophys. Res., submitted, 1984.

Zmuda, A. J., and J. C. Armstrong, The diurnal variation of the region with vector magnetic field changes associated with field-aligned currents, J. Geophys. Res., 79, 2501, 1974a.

Zmuda, A. J., and J. C. Armstrong, The diurnal flow pattern of field-aligned currents, J. Geophys. Res., 79, 4611, 1974b.

FIGURE CAPTIONS

Figure 1 — Typical DE-1 electric and magnetic field spectrograms showing the low frequency electric and magnetic field noise observed at low altitudes over the auroral zones. Note that the low frequency noise occurs over both the evening and morning auroral regions, but is almost completely absent over the polar cap.

Figure 2 — Another example of the low frequency electric and magnetic field noise during a pass about three months after the event in Figure 1. Very similar low frequency noise spectrums are observed on essentially all low altitude passes over the auroral zones.

Figure 3 — A magnetic meridian plane plot of all of the low frequency noise events detected by DE-1 over a two-year period. The noise occurs continuously along the auroral L-shells at radial distances up to about 2 R_E. Note the tendency for the latitudinal width to increase with decreasing altitude, as though the noise is spreading out and propagating downward from a source at high altitudes.

Figure 4 An invariant-latitude/magnetic-local-time plot of all of the low frequency noise events detected by DE-1 over a two-year period. The noise occurs at essentially all local times. The gaps in the early morning and early afternoon are in regions where no low altitude data are available.

Figure 5 A comparison of the DE-1 low energy, 56 to 13,206 eV, electron measurements with the low frequency noise observed on a low altitude pass over the southern polar region on October 25, 1981. The region of intense low frequency noise (shaded) occurs in regions of low energy electron fluxes and field-aligned currents typical of the auroral zone.

Figure 6 Another example showing the relationship between the low frequency magnetic noise, shown in the top panel, and the low energy electron measurements, shown in the bottom three panels. The low frequency noise is closely related to the region of field-aligned currents linking the auroral zone and the distant magnetosphere.

Figure 7 An example of simultaneously measured electric and magnetic field spectrums for a low frequency noise event detected by DE-1. Note that most of the energy in the spectrum is concentrated at frequencies below the 0^+ cyclotron frequency, f_{c0+}. The top panel shows the magnetic to electric field ratio in terms of the index of refraction, cB/E, and the conductivity, $B/(\mu_0 E)$.

Figure 8 Another set of spectrums comparable to Figure 7. Note that the magnetic spectrum has a distinct drop in intensity slightly below the 0^+ cyclotron frequency, f_{c0+}.

Figure 9 A scatter plot of the magnetic to electric field ratio, expressed as either cB/E or $B/(\mu_0 E)$, as a function of altitude. Note the strong tendency for the magnetic to electric field ratio to decrease with increasing radial distance.

Figure 10 A plot of the electric and magnetic field amplitudes, E_x and B_z, the relative phase ϕ, and correlation coefficient ρ, for a low frequency noise event detected over the southern auroral zone. Note the relatively high correlation coefficient between the

E_x and B_z fields and the square wave spin modulation pattern in the phase plot. These measurements show that the fluctuations in the E_x and B_z fields are closely correlated, with the Poynting flux directed downward toward the Earth.

Figure 11 A correlation plot similar to Figure 9 for the E_x and E_z fields. Although these fields have a relatively high correlation coefficient, often greater than 50%, the phase plot does not show a square wave spin modulation pattern, indicating that the perpendicular electric field is randomly polarized.

Figure 12 An illustration showing how field-aligned currents closing through a conducting layer at the base of the ionosphere can produce closely correlated north-south electric and east-west magnetic fields. The magnetic to electric field ratio is determined by the height-integrated Pedersen conductivity, Σ_p.

Figure 13 A model of the Alfven index of refraction as a function of radial distance for comparison with Figure 9. The electron density profile used in this model is taken from Persoon et al. [1983]. The upper limit

assumes that the plasma is entirely O^+, and the lower limit assumes a transition from H^+ to O^+ at about 1.4 R_E. Also shown is the magnetic to electric field ratio for the quasi-static model with $E_{\parallel} = 0$. The limits on ω_p are from Horwitz et al. [1978].

Figure 14 A plot of the O^+ cyclotron frequency as a function of altitude showing how a left-hand polarized Alfven reflected from the ionosphere would be absorbed by ion cyclotron damping at the O^+ cyclotron frequency. This energy absorption could heat O^+ ions, possibly producing ion conics and other non-thermal ion distributions.

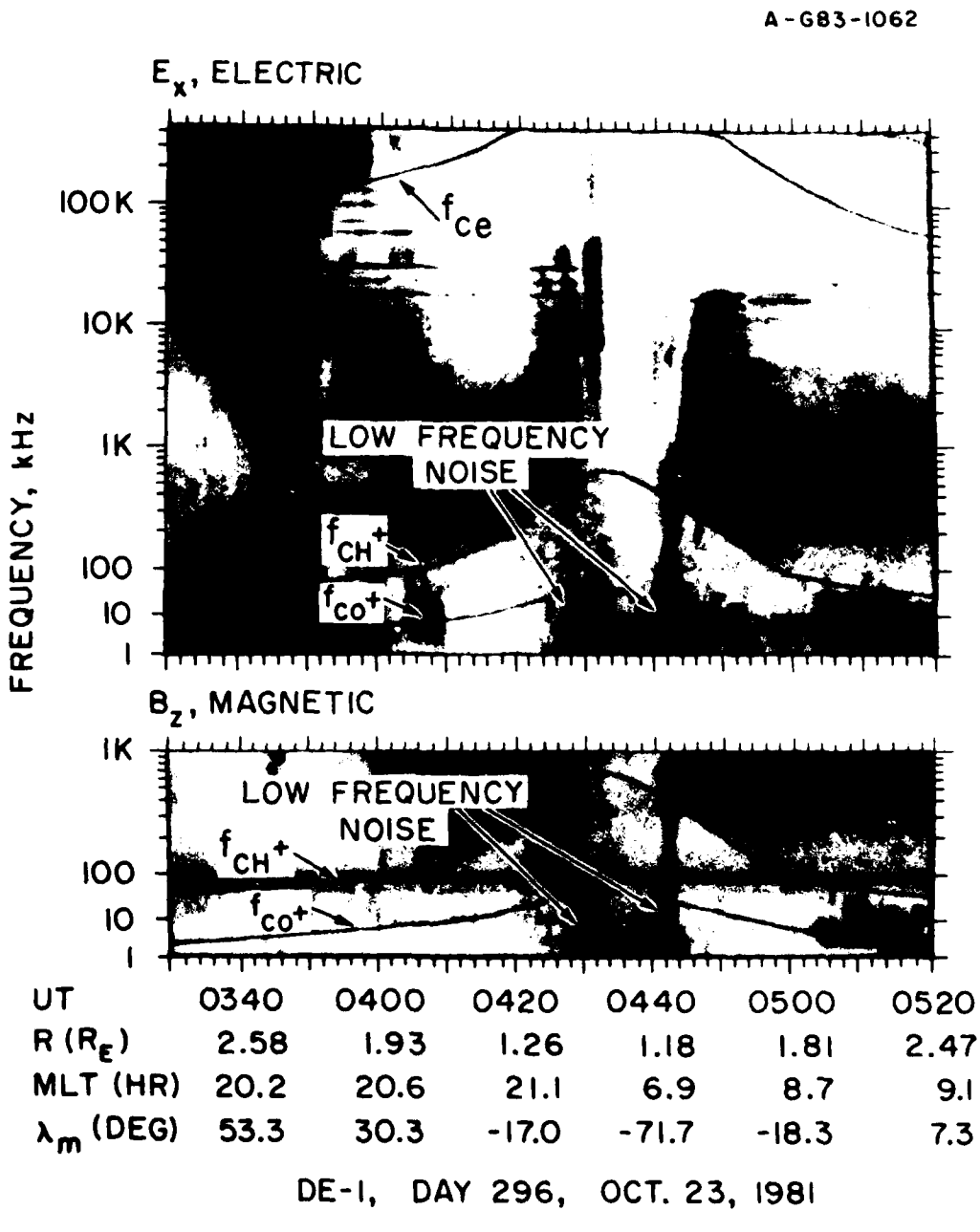
A-G83-1062
E_x, ELECTRIC
100K
10K
1K
100
10
1
f_{ce}
LOW FREQUENCY NOISE
f_{CH^+}
f_{CO^+}
FREQUENCY, kHz
B_z, MAGNETIC
1K
100
10
1
LOW FREQUENCY NOISE
f_{CH^+}
f_{CO^+}
UT 0340 0400 0420 0440 0500 0520
R (R_E) 2.58 1.93 1.26 1.18 1.81 2.47
MLT (HR) 20.2 20.6 21.1 6.9 8.7 9.1
λ_m (DEG) 53.3 30.3 -17.0 -71.7 -18.3 7.3
DE-1, DAY 296, OCT. 23, 1981

Figure 1

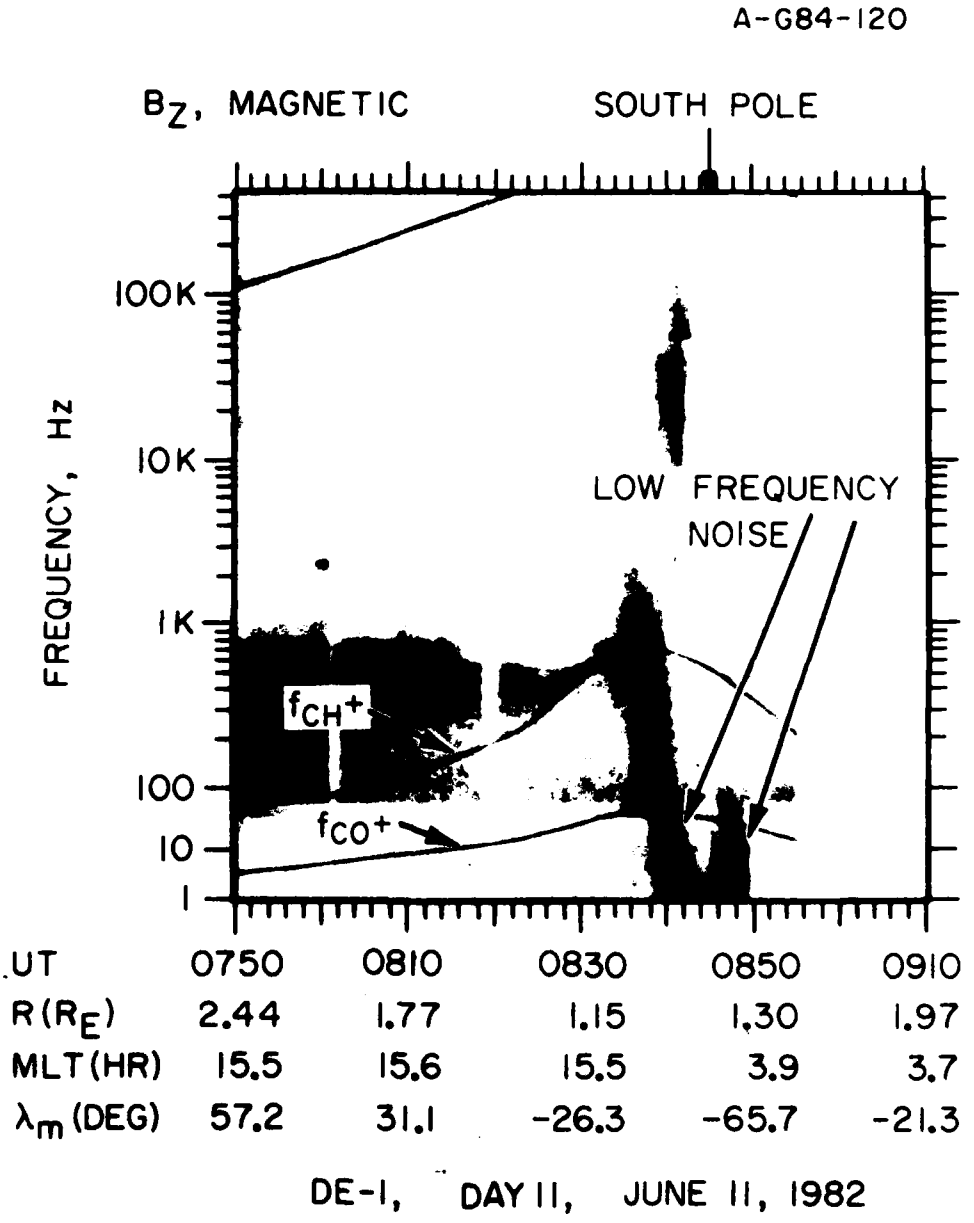
A-G84-120
B_Z, MAGNETIC
SOUTH POLE
100K
10K
1K
100
10
1
FREQUENCY, Hz
LOW FREQUENCY
NOISE
f_{CH^+}
f_{CO^+}
UT 0750 0810 0830 0850 0910
R(R_E) 2.44 1.77 1.15 1.30 1.97
MLT(HR) 15.5 15.6 15.5 3.9 3.7
λ_m(DEG) 57.2 31.1 -26.3 -65.7 -21.3
DE-1, DAY 11, JUNE 11, 1982

Figure 2

A-G83-1064-1

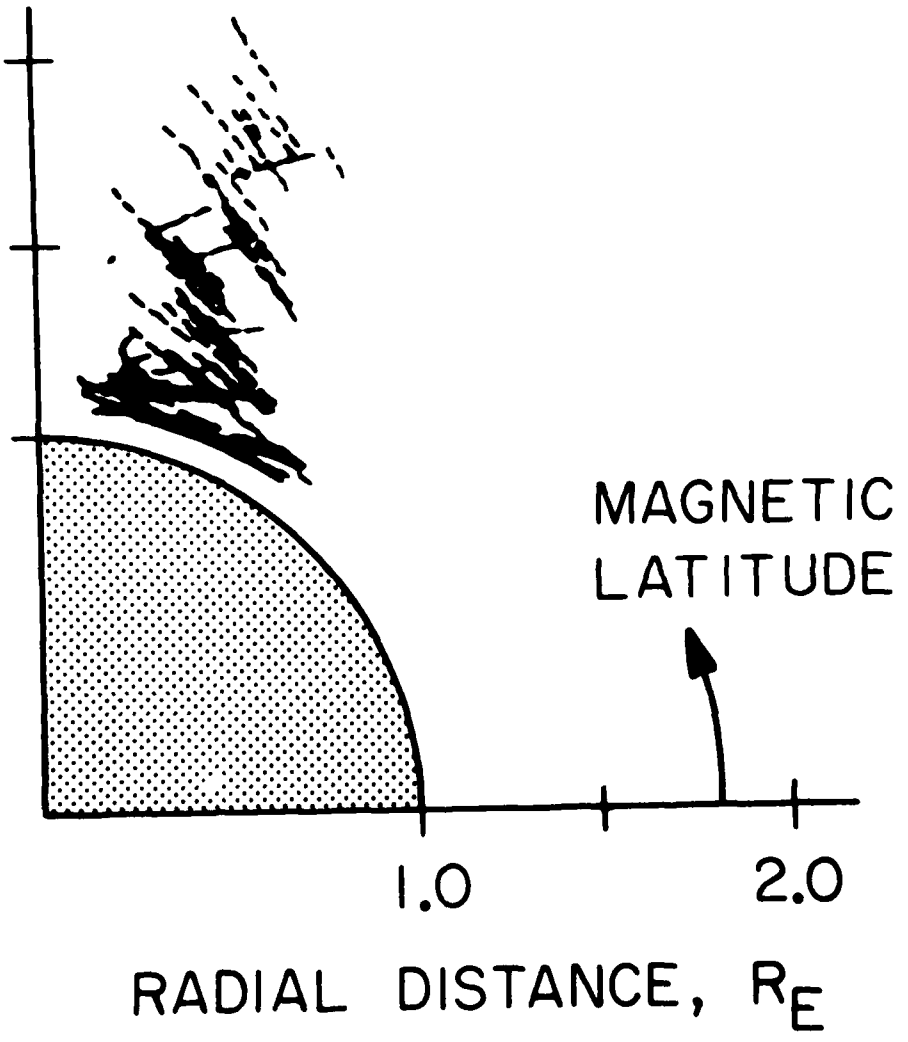

Figure 3

A-G83-1063-2

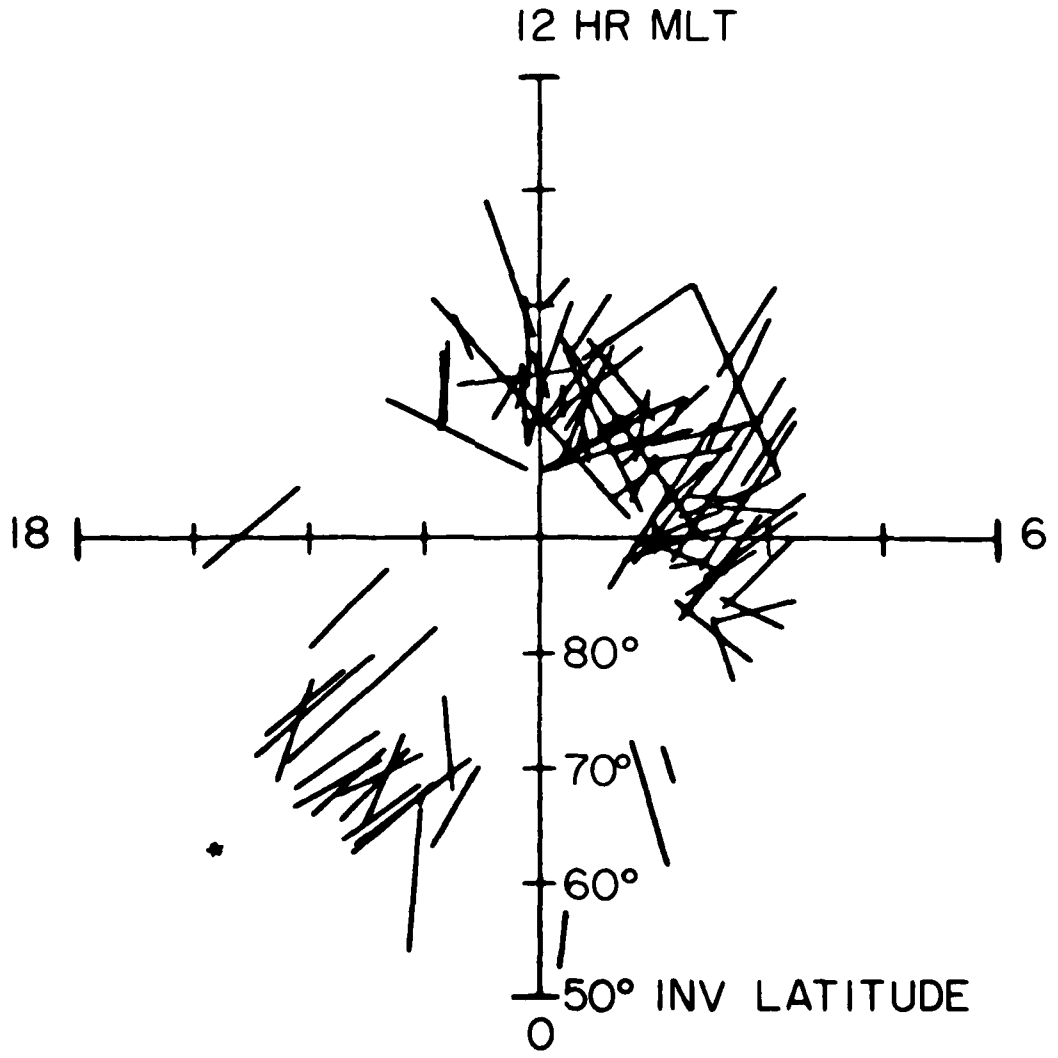

Figure 4

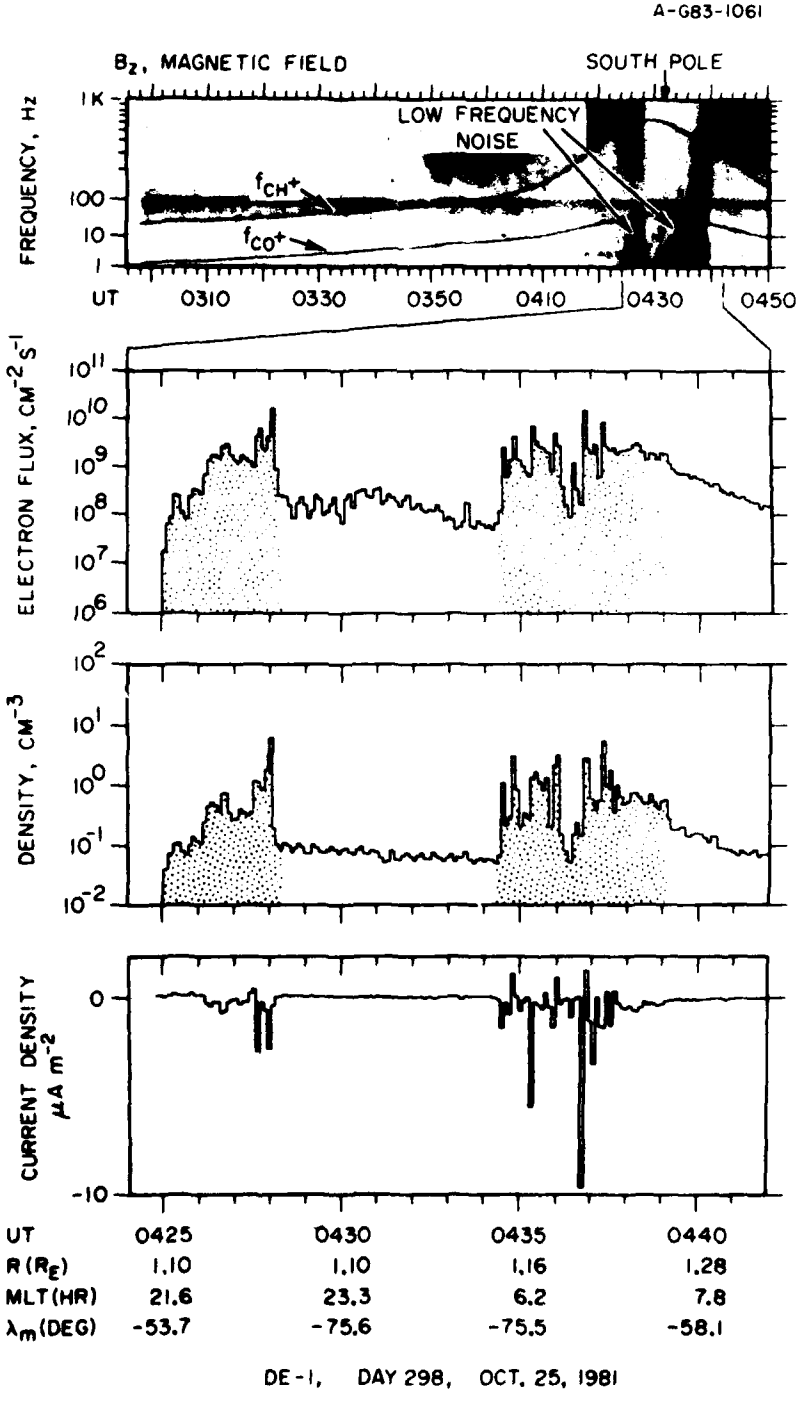
A-G83-1061
B_z, MAGNETIC FIELD
SOUTH POLE
FREQUENCY, Hz
1K
100
10
1
LOW FREQUENCY NOISE
f_{CH^+}
f_{CO^+}
UT
0310
0330
0350
0410
0430
0450
ELECTRON FLUX, $CM^{-2}S^{-1}$
10^{11}
10^{10}
10^9
10^8
10^7
10^6
DENSITY, CM^{-3}
10^2
10^1
10^0
10^{-1}
10^{-2}
CURRENT DENSITY $\mu A\ m^{-2}$
0
-10
UT 0425 0430 0435 0440
R(R_E) 1.10 1.10 1.16 1.28
MLT(HR) 21.6 23.3 6.2 7.8
λ_m(DEG) -53.7 -75.6 -75.5 -58.1
DE-1, DAY 298, OCT. 25, 1981

Figure 5

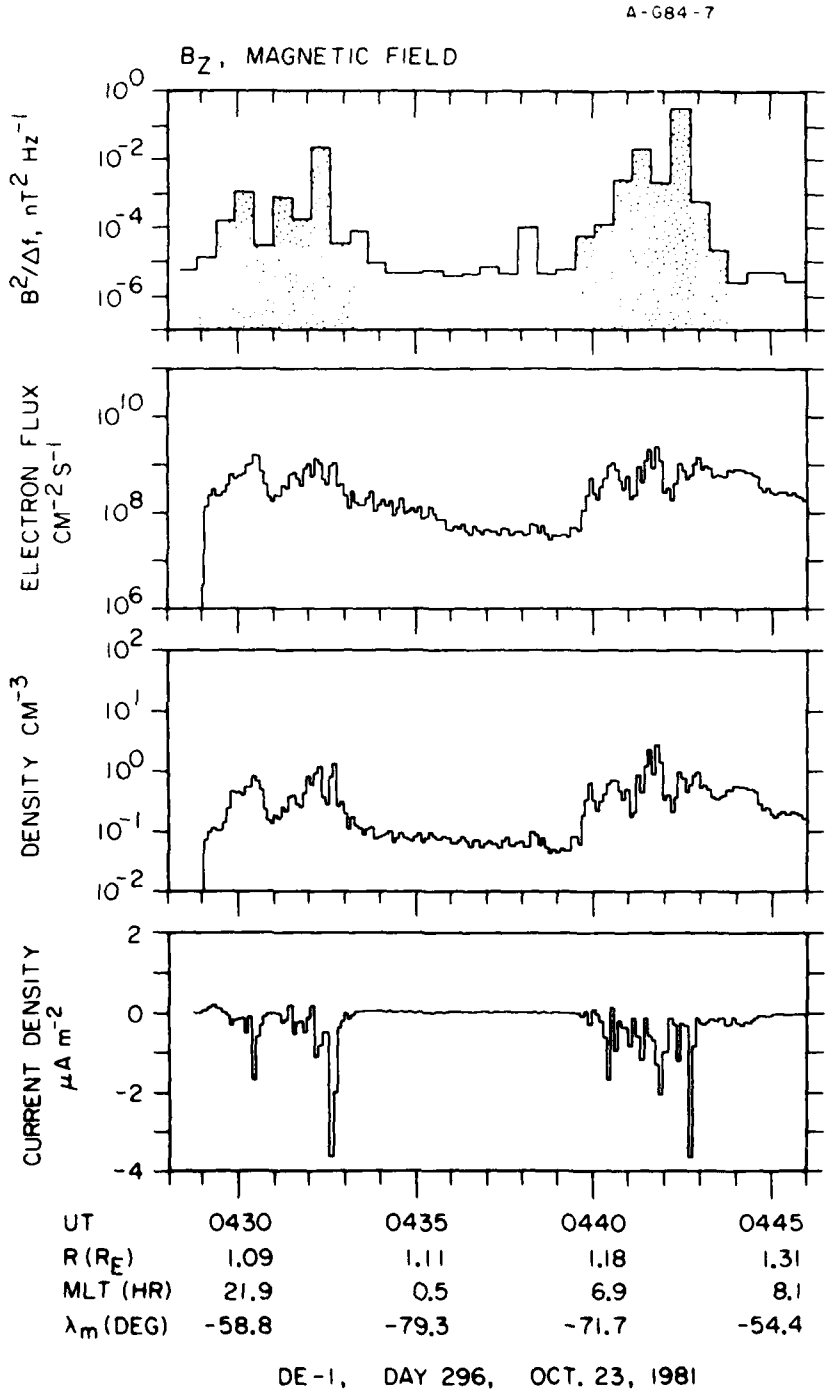
A-G84-7
B_Z, MAGNETIC FIELD
$B^2/\Delta f$, $nT^2\ Hz^{-1}$
10^0
10^{-2}
10^{-4}
10^{-6}
ELECTRON FLUX
$CM^{-2}S^{-1}$
10^{10}
10^8
10^6
DENSITY CM^{-3}
10^2
10^1
10^0
10^{-1}
10^{-2}
CURRENT DENSITY
$\mu A\ m^{-2}$
2
0
-2
-4
UT 0430 0435 0440 0445
R (R_E) 1.09 1.11 1.18 1.31
MLT (HR) 21.9 0.5 6.9 8.1
λ_m (DEG) -58.8 -79.3 -71.7 -54.4
DE-1, DAY 296, OCT. 23, 1981

Figure 6

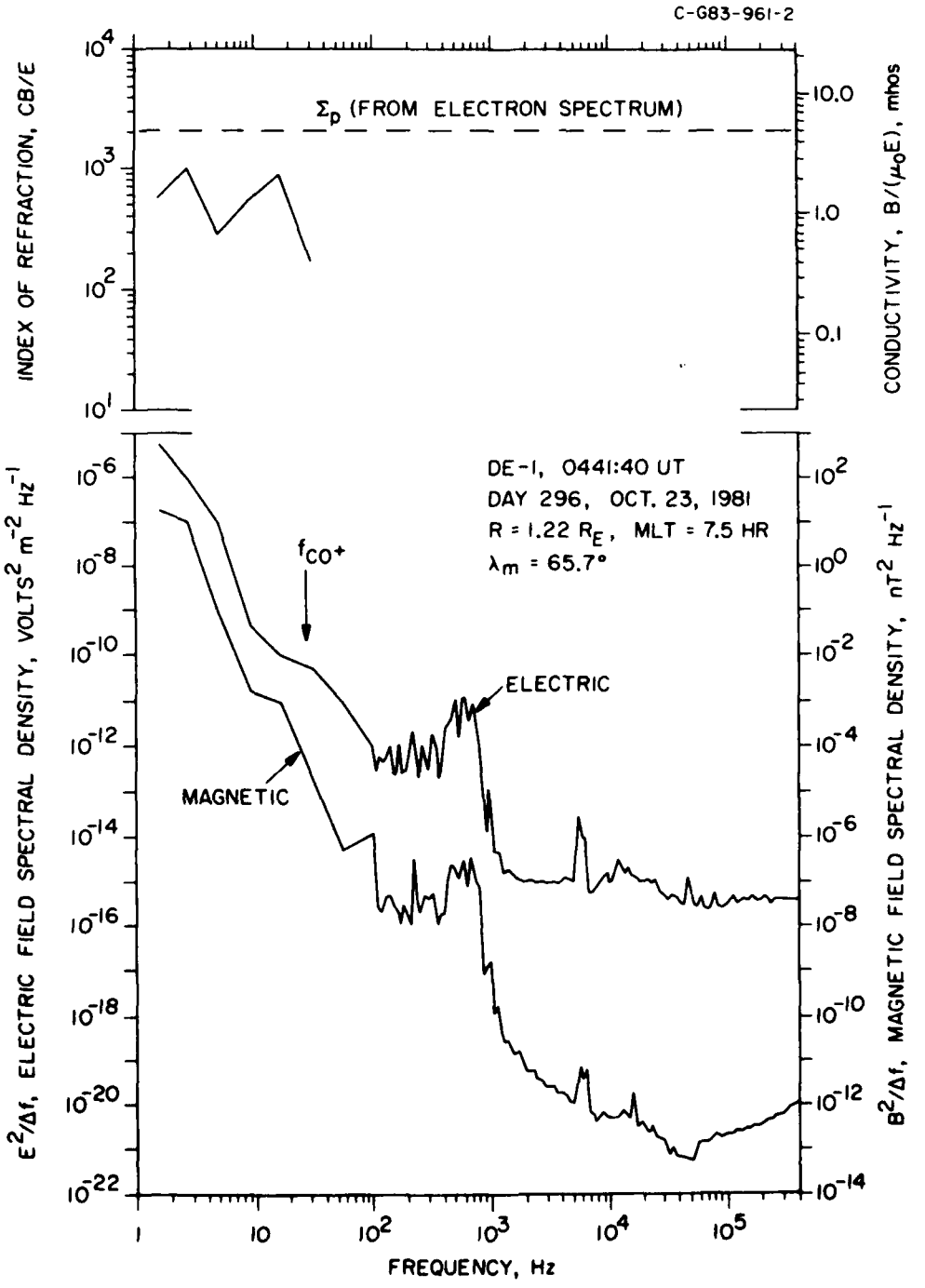
C-G83-961-2
INDEX OF REFRACTION, CB/E
CONDUCTIVITY, B/(μ0E), mhos
Σp (FROM ELECTRON SPECTRUM)
DE-1, 0441:40 UT
DAY 296, OCT. 23, 1981
R = 1.22 RE, MLT = 7.5 HR
λm = 65.7°
fCO+
ELECTRIC
MAGNETIC
E2/Δf, ELECTRIC FIELD SPECTRAL DENSITY, VOLTS2 m-2 Hz-1
B2/Δf, MAGNETIC FIELD SPECTRAL DENSITY, nT2 Hz-1
FREQUENCY, Hz

Figure 7

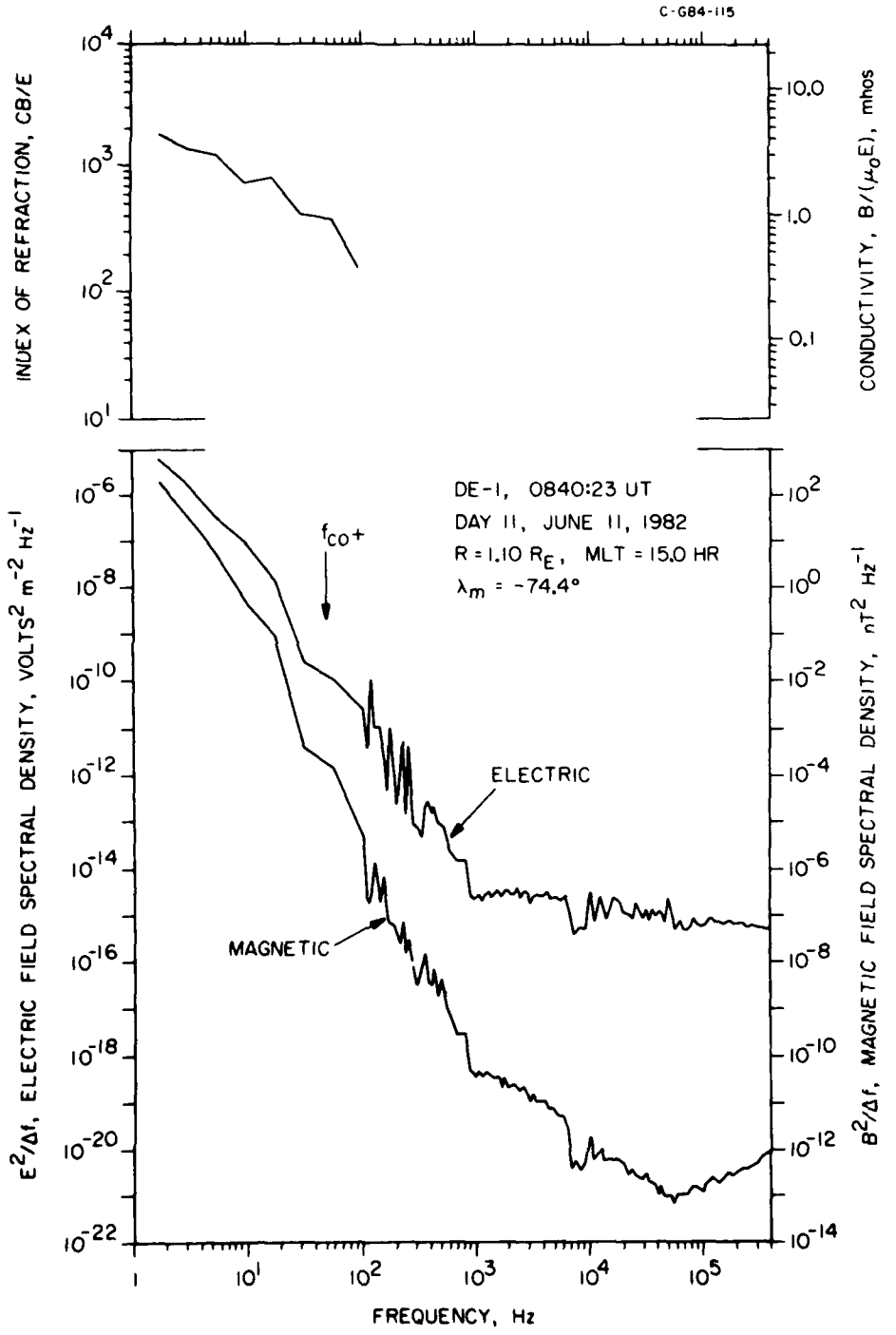
C-G84-115
INDEX OF REFRACTION, CB/E
CONDUCTIVITY, B/(μ0E), mhos
DE-1, 0840:23 UT
DAY 11, JUNE 11, 1982
R = 1.10 RE, MLT = 15.0 HR
λm = -74.4°
fco+
ELECTRIC
MAGNETIC
E²/Δf, ELECTRIC FIELD SPECTRAL DENSITY, VOLTS² m⁻² Hz⁻¹
B²/Δf, MAGNETIC FIELD SPECTRAL DENSITY, nT² Hz⁻¹
FREQUENCY, Hz

Figure 8

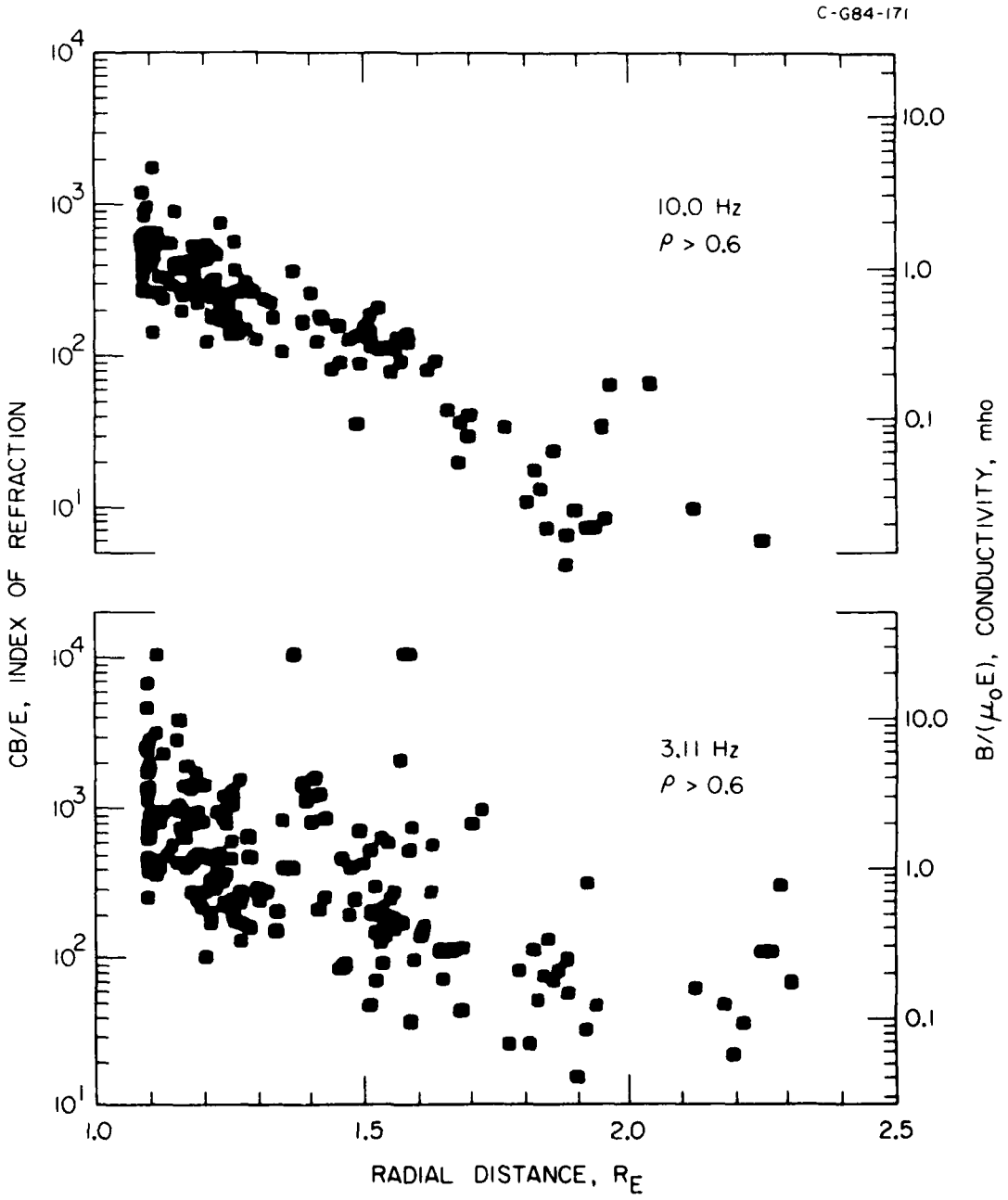
C-G84-171
10.0 Hz
ρ > 0.6
3.11 Hz
ρ > 0.6
CB/E, INDEX OF REFRACTION
B/(μ0E), CONDUCTIVITY, mho
RADIAL DISTANCE, RE
1.0
1.5
2.0
2.5
10.0
1.0
0.1

Figure 9

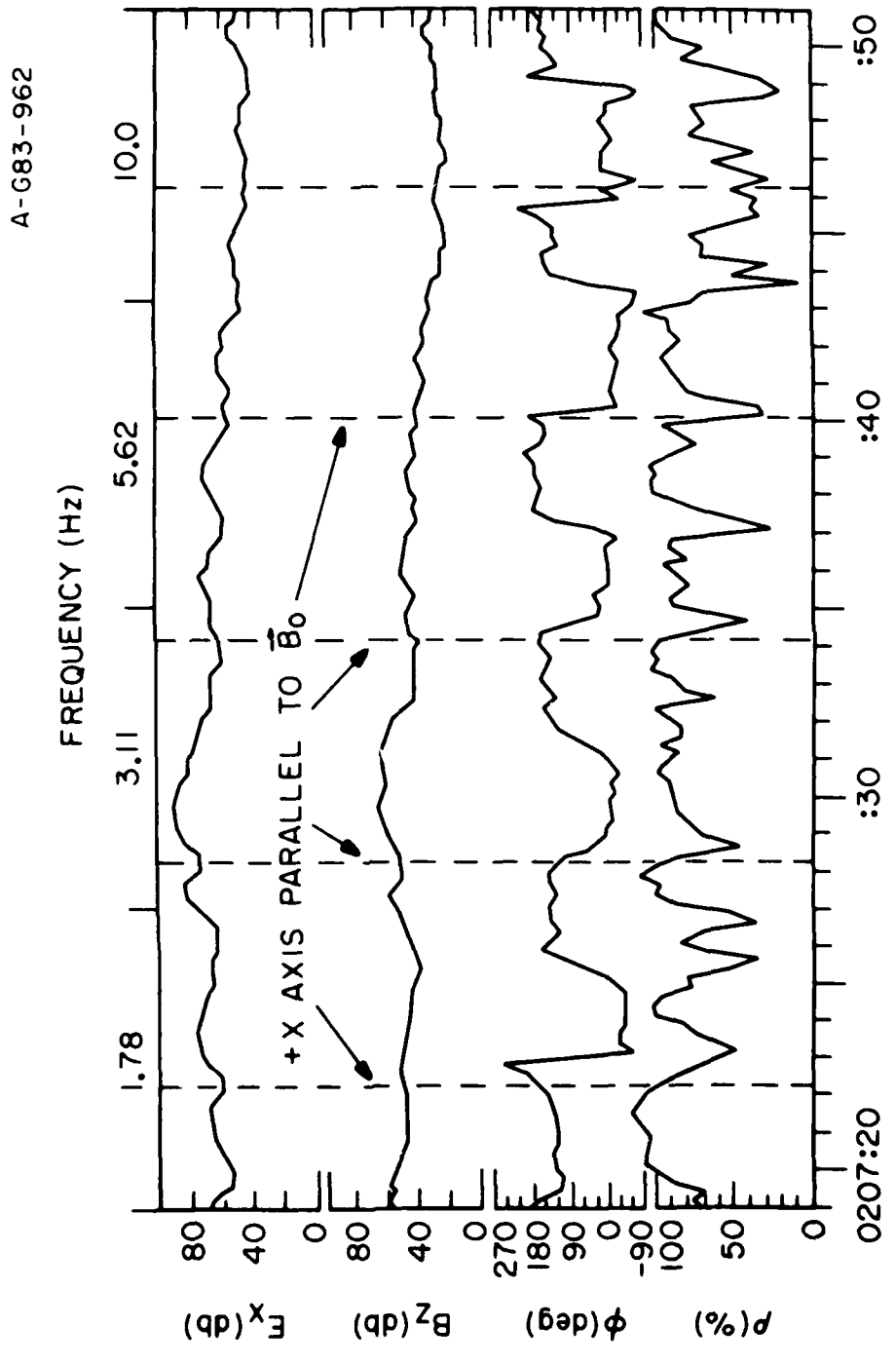
A-G83-962
FREQUENCY (Hz)
1.78
3.11
5.62
10.0
+X AXIS PARALLEL TO $\vec{B}_o$
DE-1, DAY 267, SEPT. 24, 1981
0207:20
:30
:40
:50
E_X(db)
B_Z(db)
ϕ(deg)
ρ(%)
80
40
0
80
40
0
270
180
90
0
-90
100
50
0

Figure 10

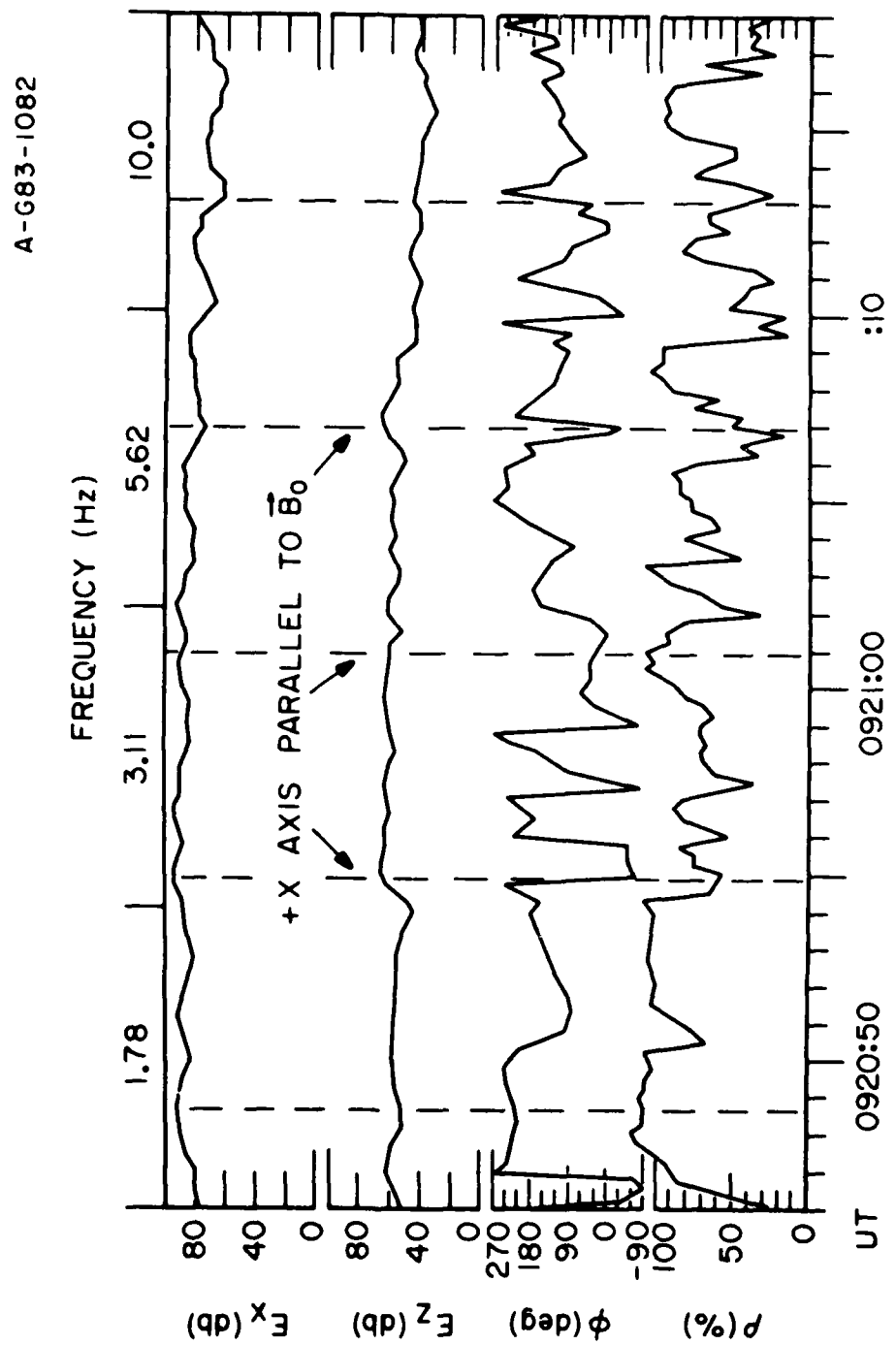
A-G83-1082
FREQUENCY (Hz)
1.78
3.11
5.62
10.0
+X AXIS PARALLEL TO $\vec{B}_0$
DE-1, DAY 299, OCT. 26, 1981
UT 0920:50
0921:00
:10
80
40
0
80
40
0
270
180
90
0
-90
-100
50
0
E_X (db)
E_Z (db)
ϕ (deg)
ρ (%)

Figure 11

A-G83-970-2

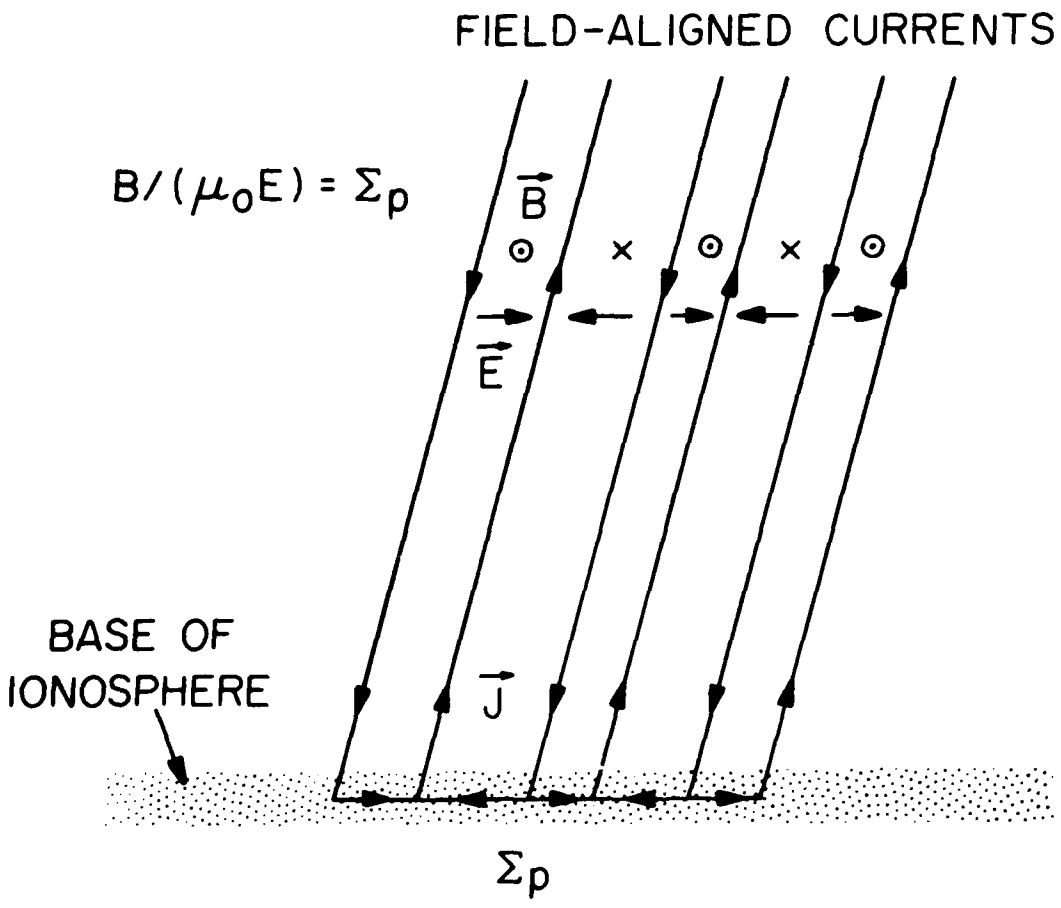

Figure 12

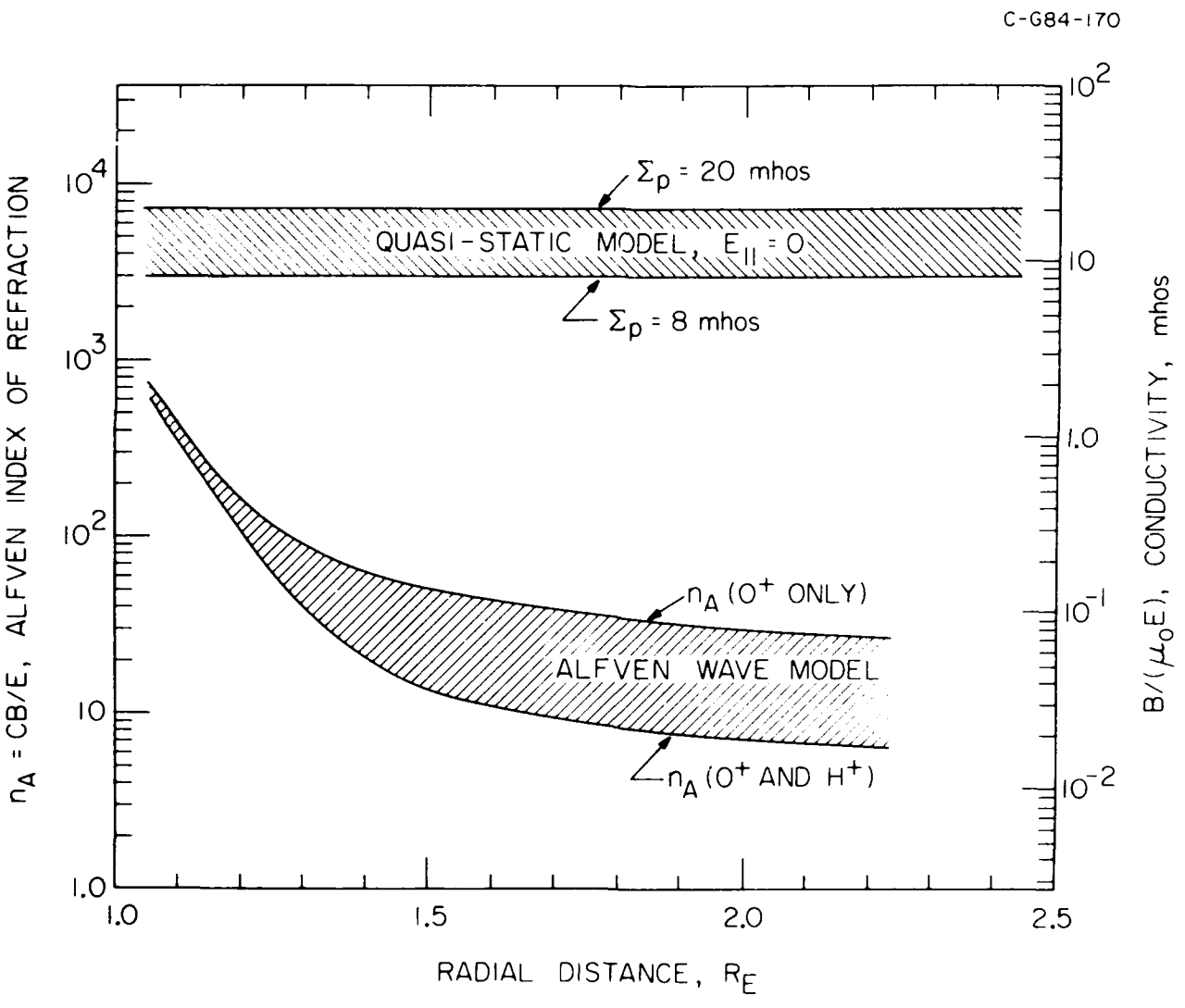
C-G84-170
Σ_p = 20 mhos
QUASI-STATIC MODEL, $E_{||}$ = 0
Σ_p = 8 mhos
n_A (O^+ ONLY)
ALFVEN WAVE MODEL
n_A (O^+ AND H^+)
n_A = CB/E, ALFVEN INDEX OF REFRACTION
$B/(\mu_0 E)$, CONDUCTIVITY, mhos
RADIAL DISTANCE, R_E
10^4
10^3
10^2
10
1.0
10^2
10
1.0
10^{-1}
10^{-2}
1.0
1.5
2.0
2.5

Figure 13

A-G83-943-2

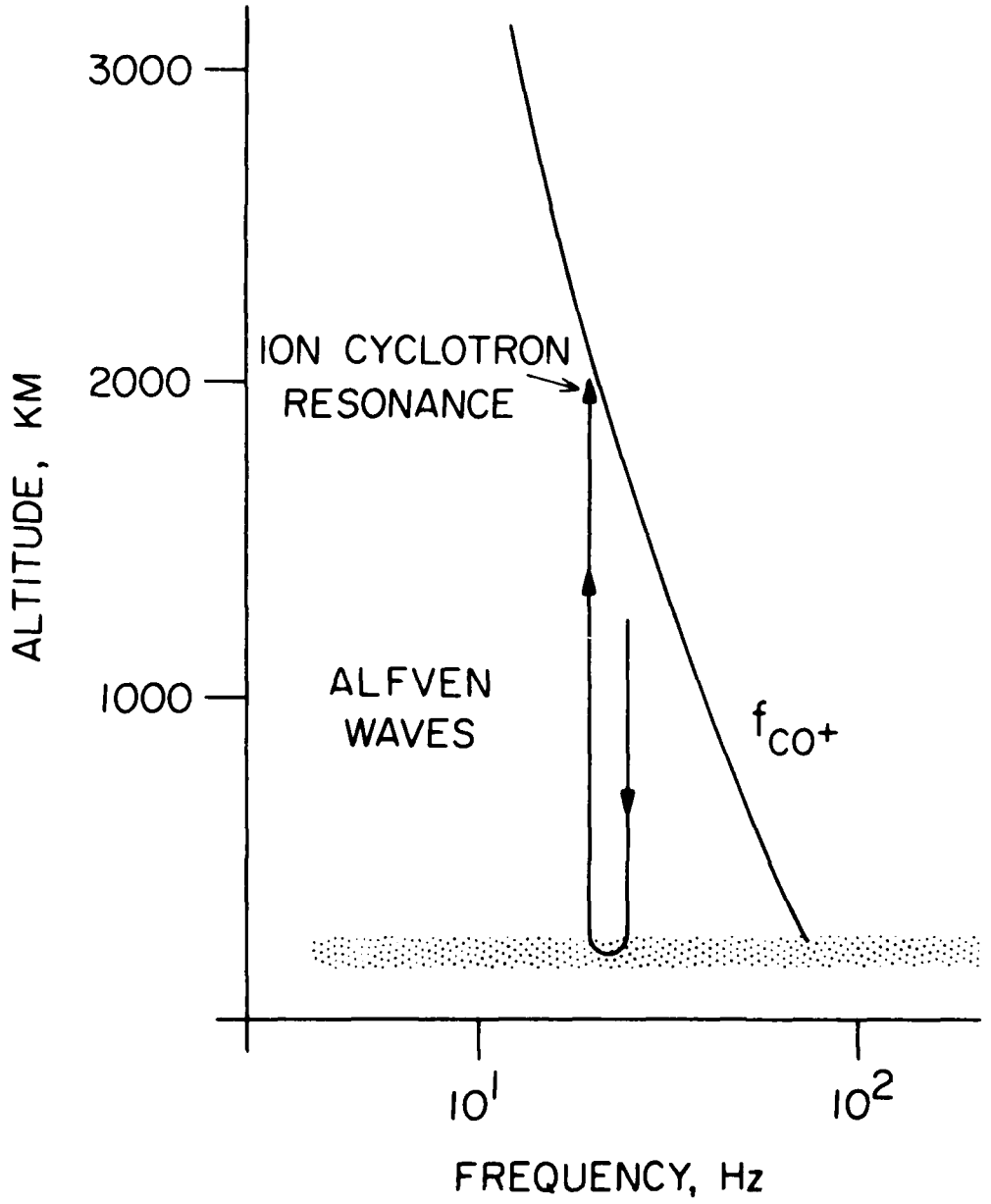

Figure 14